INTERNATIONAL JOURNAL FOR NUMERICAL METHODS IN FLUIDS, VOL. 9, 623–650 (1989)

QUANTUM PHENOMENA IN NUMERICAL WAVE PROPAGATION

ROBERT VICHNEVETSKY

Department of Computer Science, Rutgers University, New Brunswick, NJ 08903, U.S.A.

SUMMARY

The analysis of wave propagation in computing domains where hyperbolic equations are approximated with finite differences has revealed surprising analogies between this subject and quantum mechanics. The first part of this paper consists of a review of the corresponding phenomena and of their description with known results from numerical analysis and wave propagation theory. We then introduce a new formalism, containing a finite difference analogue of the classical Schrödinger equation, which describes the ensemble of those phenomena. The validity of the new formalism is verified by its agreement with known theoretical results in numerical wave propagation (it contains in fact many of those results) as well as with new data obtained in numerical experiments with monochromatic waves which display properties similar to those of Schrödinger's wavefunction for the quantum mechanics description of the equivalent experiments with physical particles. While the results of this paper are derived in the context of wave propagation in computing domains, they remain applicable to similar aspects of wave propagation in other (physical) periodic structures.

KEY WORDS Numerical analysis Wave propagation Hyperbolic equations Quantum mechanics

1. INTRODUCTION

Recent analyses of wave propagation in computing domains where hyperbolic equations are approximated with finite differences have brought to the fore striking (and somewhat surprising) analogies between the corresponding phenomena and those of quantum mechanics. This has pointed towards a possible explanation of those phenomena in a manner similar to the description of physical particles with Schrödinger's theory. It is this question which is investigated in this paper: we will find, as was expected, that one may indeed develop such a new formalism (or theory) to explain the observed phenomena while agreeing with their known properties from standard wave propagation theory. By contrast with classical quantum mechanics which applies only to atomic-scale phenomena, the new formalism describes 'large-scale' phenomena: the corresponding quanta are related to the finite size of the mesh increments which discretize the computing domain.

Those computing domains for which the theory is developed are only to be considered as examples. The essence of the new results applies identically to the description of similar aspects of wave propagation in many other (physical) periodic structures (this will be reported separately). What atomic physics and numerical wave propagation have in common is the presence of quantized variables (energy levels in the former case, spatial position in the latter). This evidently has the effect of generating wave phenomena of a certain kind, of a wavelength directly related to the quantization steps. In quantum mechanics, Schrödinger's equation establishes a direct

0271–2091/89/060623–28$14.00

Received 7 August 1987
Revised 8 August 1988

relationship between the Hamiltonian corresponding to the motion of an elementary mass particle and its wave equivalent (also described by de Broglie's relation). We will find that a similar relationship may be established in the case of numerical wave propagation. This will be achieved by first likening wave packets in computing domains to mass particles moving in a potential field, then by deriving from the corresponding Hamiltonian an equation (a finite difference analogue of Schrödinger's equation) whose solution is simply related to the original wave.

Part of the theoretical foundation for the analysis of this paper is of course that concerning wave propagation in difference schemes: numerical wave propagation in piecewise uniform grids has been reasonably well described in the literature (e.g. References 1–10). By contrast, published results concerning wave propagation in non-uniform grids (a topic which shall hold a central place in this paper) are much fewer. One of the first analyses in that direction was that of Giles and Thompkins.[11] This question was also examined briefly by Trefethen,[4] and by Chin and Hedstrom[12] with special attention to the problem of scattering. Results on propagation in non-uniform grids which are most relevant to the present study have been given in Reference 13 by the present author.

2. WAVE PROPAGATION IN SPACE-DISCRETIZED DOMAINS

What must be the simplest model of wave propagation in discrete-space structures is that displayed by solutions to the system of difference–differential equations

$$\frac{\mathrm{d}u_n}{\mathrm{d}t} = -c\left(\frac{u_{n+1}-u_{n-1}}{\delta_n+\delta_{n+1}}\right), \quad n = 0, \pm 1, \pm 2, \ldots, \quad c = \text{constant} > 0, \tag{1}$$

where the u_n belong to a variable taking its values at a set $\{x_n\}$ of discrete points on the x-axis,

$$\ldots < x_{n-1} < x_n < x_{n+1} < \ldots, \tag{2}$$

and $\{\delta_n\} = \{x_n - x_{n-1}\}$ is the corresponding set of spatial increments, which shall in general be dependent of n.

It may of course be recognized that (1) is obtained when the simple scalar hyperbolic equation

$$\frac{\partial U}{\partial t} + c\frac{\partial U}{\partial x} = 0; \qquad U = U(x,t), \tag{3}$$

is approximated numerically with central finite differences on the mesh (2), with the u_n interpreted as approximations of $U(x,t)$ at the nodes. This remark, however, is not essential for the following developments, other than for the fact that the analogy of the discrete model with the approximation of a hyperbolic equation provides concepts which are occasionally useful.

The l_2-norm of $u \equiv \{u_n\}$,

$$\|u\|_2 \equiv \left(\sum_{n=-\infty}^{\infty} \frac{(\delta_n+\delta_{n+1})}{2} u_n^2\right)^{1/2}, \tag{4}$$

is easily proven (when it is finite, i.e. when u is in a Hilbert space) to be a strict invariant when u is a solution of the Cauchy problem for (1).

Numerical computations are discrete in time as well as in space. The integration of (1) is to be implemented by means of some discrete stepping method (the Crank–Nicolson method in the examples that illustrate this paper). But save for minor changes in notations and definitions, those theoretical results concerning propagation and reflection which are derived with the semidiscrete

model and which can be quantified with quadratic norms (as will be the case almost everywhere in the sequel) do remain strictly applicable to the fully discrete calculations (formal proofs of this property may be found in References 9, 14 and 15). We shall thus, for simplicity, limit our analysis to that of the semidiscrete case.

It may be shown, by a simple relabelling of variables, that (1) is not only a difference analogue of (3) but also of the standard second-order wave equation[10]

$$\frac{\partial^2 U}{\partial t^2} - c^2 \frac{\partial^2 U}{\partial x^2} = 0. \tag{5}$$

Thus, as does this equation, (1) admits bidirectional wave propagation.

3. MONOCHROMATIC WAVES

We shall assume that, except for a finite number of points of discontinuity, δ_n varies continuously and slowly with respect to n, and that, accordingly, the discrete sequence $\{\delta_n\}$ may be embedded in a continuous function $\delta(x)$ which varies slowly with respect to x. Computing domains where (1) applies constitute dispersive media with respect to wave propagation. In those regions where there are no mesh size discontinuities, (1) admits wavelike sinusoidal solutions of the form[13,16]

$$u_n(t) = u(x_n, t) = \alpha(x_n, t)\exp\left[\mathrm{i}\left(\omega t + \int^{x_n} \xi(x)\,\mathrm{d}x \right) \right], \tag{6}$$

where the frequency ω is a constant (these are monochromatic solutions); $\alpha(x, t)$ is an amplitude function, assumed to vary slowly with respect to both the mesh increments and the individual oscillations of the wave described by $\exp(\mathrm{i}\int \xi\,\mathrm{d}x)$; and $\xi(x)$ is a local wave number.

The frequency and wave number are linked by the dispersion relation, which is position-dependent,

$$\omega = -\frac{c}{\delta(x)} \sin(\xi(x)\delta(x)), \tag{7}$$

and this relation implies that $\xi(x)$ varies slowly with respect to x.

When u is a monochromatic solution (of the form (6)), then $\| u \|_2^2$, the square of its l_2-norm, may be approximated by the integral

$$\| u \|_2^2 = \int |u(x, t)|^2\,\mathrm{d}x = \int \alpha^2(x, t)\,\mathrm{d}x = \text{constant}. \tag{8}$$

It is a standard result in classical wave propagation theory (see e.g. Reference 16, Chapter 11) that the displacement of the conserved quantity $|u(x, t)|^2$ (the integrand of (8)) takes place locally at the group velocity G defined by

$$G = -\,\mathrm{d}\omega/\mathrm{d}\xi,$$

where $\omega(\xi)$ is the dispersion relation. Whence, with (7) (see Figure 1),

$$G(\xi, x) = c\cos(\xi(x)\delta(x))$$

or

$$G_{\pm}(\omega, x) = \pm c\left[1 - \left(\frac{\omega\delta(x)}{c} \right)^2 \right]^{1/2}, \tag{9}$$

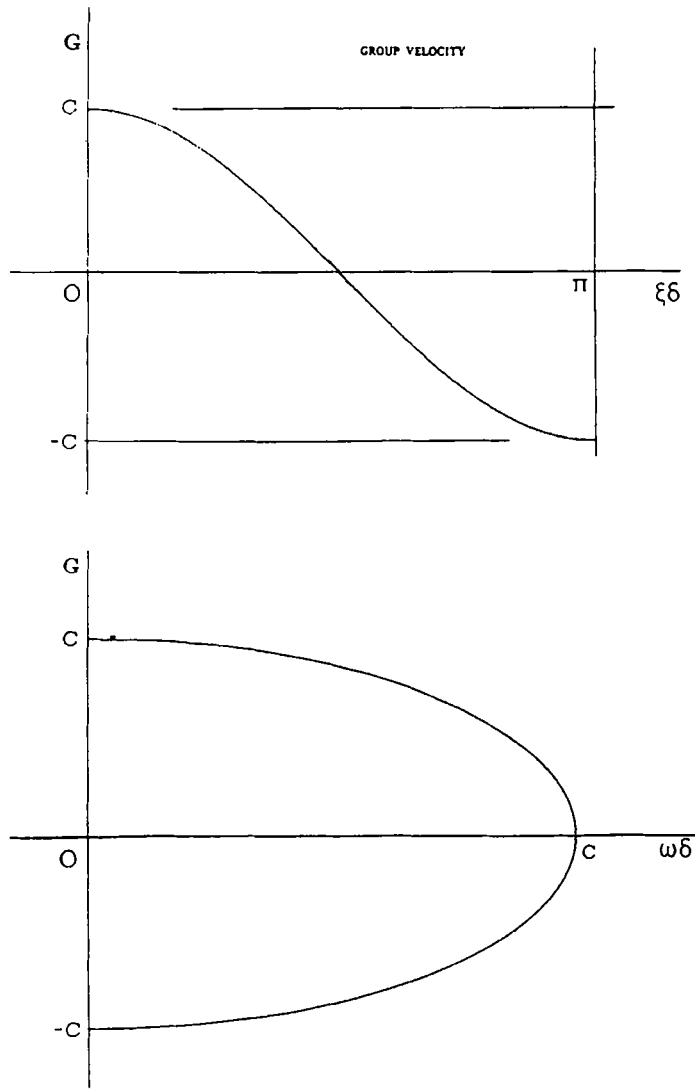

Figure 1. (a) Group velocity versus δ and wave number. (b) Group velocity versus δ and frequency

where the two signs ($\pm$) correspond to right-going and left-going waves respectively: to each ω satisfying

$$|\omega| < \omega_c = c/\delta \tag{10}$$

(where ω_c is called the cut-off frequency) there correspond two group velocities, equal in magnitude but of opposite sign, approximating the wave speed of the two solutions of (5). The invariance of (8) and the fact that $|u(x, t)|^2$ propagates at the group velocity may be combined to produce the conservation law for monochromatic solutions,[11, 13, 16]

$$\frac{\partial |u|^2}{\partial t} + \frac{\partial}{\partial x}(G|u|^2) = 0 \quad \text{or} \quad \frac{\partial \alpha^2}{\partial t} + \frac{\partial}{\partial x}(G\alpha^2) = 0, \tag{11}$$

which is to hold separately for right-going waves ($G = G_+, u = u_+, \alpha = \alpha_+$) and left-going waves ($G = G_-, u = u_-, \alpha = \alpha_-$). The expressions

$$G|u|^2 = G\alpha^2 \tag{12}$$

which appear in those equations represent 'flows' of $|u(x,t)|^2 = \alpha^2(x,t)$. (An expression which is equivalent to (11) may be found in Giles nd Thompkins,[11] who obtained it by doing an asymptotic analysis, in Fourier space, of a numerical algorithm similar to (1).)

4. A FIRST ANALOGY WITH MECHANICS

We will show that the laws which describe the propagation of monochromatic waves contain analogies with those of classical and quantum mechanics. The first part of the analogy (that with classical mechanics) may be brought to light by analysing the dynamics of $\alpha(x,t)$ in (6)—i.e. ignoring the internal oscillations described by $\exp(i\int \xi\,dx)$; the analogy with quantum mechanics comes later, when those internal oscillations will be reintroduced in the analysis.

A simple device will consist of labelling the quantity defined by (8) with the symbol m and calling it the wave mass:

$$m \equiv \int |u(x,t)|^2\,dx = \int |\alpha(x,t)|^2\,dx = \text{constant}. \tag{13}$$

We also define a wave kinetic energy

$$T(t) = \int \frac{G^2}{2}|u(x,t)|^2\,dx = \int \mathscr{T}|u(x,t)|^2\,dx \qquad \left(\mathscr{T}(\omega,x) = \frac{G^2(\omega,x)}{2}\right) \tag{14}$$

and a wave potential energy

$$V(t) = \int \frac{(\omega\delta)^2}{2}|u(x,t)|^2\,dx = \int \mathscr{V}|u(x,t)|^2\,dx \qquad \left(\mathscr{V}(\omega,x) = \frac{(\omega\delta(x))^2}{2}\right), \tag{15}$$

where $\mathscr{T}$ and $\mathscr{V}$ are the corresponding specific (i.e. per unit mass) variables. We then find that the sum

$$T(t) + V(t) = \int \frac{c^2}{2}|u(x,t)|^2\,dx = \frac{c^2}{2}m \tag{16}$$

is a constant with respect to time. These relations are identical to those describing a classical, distributed mass mechanical system. One may indeed derive from the preceding the equations of motion

$$\frac{dx}{dt} = G \qquad \frac{dG}{dt} = \frac{\partial G}{\partial x}\frac{dx}{dt} = \frac{1}{2}\frac{\partial G^2}{\partial x} = -\frac{\partial \mathscr{V}}{\partial x}, \tag{17}$$

where x and G are the position and velocity of the element $|u(x,t)|^2$ of distributed mass moving in the potential field $\mathscr{V}$ (see e.g. Goldstein[17]).

5. WAVE PACKETS AND PARTICLES

Wave packets will play the role of mass particles in the analogy between numerical wave propagation and quantum mechanics. The standard, somewhat heuristic definition of a wave packet is that it consists of a monochromatic wave of a general form similar to (6), but with a support in $\dot{x}$ limited to a finite (small) number of wavelengths.

A usual form is that having a Gaussian envelope of standard deviation σ:

$$u(x) = e^{-\frac{1}{2}[(x-x_0)/\sigma]^2} e^{i\xi_0 x}. \tag{18}$$

Its Fourier transform also has a Gaussian envelope, of standard deviation $1/\sigma$:

$$\hat{u}(\xi) = \sqrt{(2\pi)}\sigma e^{-\frac{1}{2}[(\xi-\xi_0)\sigma]^2} e^{-i\xi x_0}. \tag{19}$$

It may be recognized that this is only the approximation of an ideal wave packet. Indeed, both (18) and (19) have infinite support. By contrast, we would like an ideal wave packet to be of finite support in x and of vanishingly small wave number bandwidth in ξ. But this turns out to be unfeasible and (18) is the best one can do: while not of finite support, the wave mass of (18) is nevertheless concentrated to within a negligible remainder in a finite region near x_0 in physical space and near ξ_0 in Fourier space. The product of the approximate width of the two corresponding distribution functions is of order one: this is known as the bandwidth theorem in Fourier analysis. Loosely stated, it says that this product is bounded from below by a number of order one for any function $v(x)$. Moreover, this minimum is reached by Gaussians (and only by Gaussians) of the form (18). While one cannot create ideal wave packets of finite support, (18) is the best approximation thereof one may get. When σ is reasonably large with respect to the wavelength $\lambda_0 = 2\pi/\xi_0$, then (18) approximates a wave packet of wavenumber ξ_0.

This difficulty of constructing ideal wave packets (to be used for instance to generate initial data for numerical experiments) is no different from that of defining wave packets in quantum mechanics, where elementary particles and their associated wave train are subjected to Heisenberg's uncertainty principle. This principle and the bandwidth theorem of Fourier analysis are essentially expressions of the same mathematics. In fact, our preceding discussion about wave packets is remarkably similar to discussions found in quantum mechanics texts in relation to the analytic expression of the wave equivalent of a particle.[18, 19]

The form taken by the equations for the mechanical analogue of monochromatic waves becomes particularly interesting when the analysis is restricted to wave packets. Their definition is equivalent to assuming that when u is a single wave packet, then G and δ may be approximated by constants in the integrals of Section 4. We may thus define the position of the packet as

$$X = \frac{1}{m}\int x|u(x,t)|^2\,dx. \tag{20}$$

Its velocity, wave kinetic and potential energies are then simply (to within negligible remainders)

$$\frac{dX}{dt} = G(\omega, X), \tag{21}$$

$$T = \frac{m}{2}G^2(\omega, X), \tag{22}$$

$$V = \frac{m}{2}(\omega\delta(X))^2, \tag{23}$$

and they satisfy the equations of classical mechanics for a single, pointwise particle:

$$\frac{dX}{dt} = G \qquad \frac{dG}{dt} = -\frac{1}{m}\frac{\partial V(\omega, X)}{\partial X}. \tag{24}$$

It may be noted that these equations become identical to (17) if we let $m = 1$ here and interpret (17) as describing the configuration space of a single wave packet of unit mass. We shall use the

present notations to describe both in the sequel; which is to be meant will be clear from the context.

Figure 2 gives the results of a first numerical experiment: a right-going wave packet (or 'particle') arrives from the left (where δ = constant) into a region where the mesh size—and the potential—are in the shape of a smooth, gradual increase (Figure 3). The particle climbs the hill up to the point where its total energy equals the potential energy (i.e. where its kinetic energy equals zero), then returns to the left with a symmetrical trajectory. What this example illustrates is a process of internal reflection. When (1) is used as a numerical approximation of (3), then this internal reflection process is entirely parasitic, since nothing of the sort is present in solutions of the original equation.

There are applications in computing, for example in the implementation of large aerodynamic codes, where a locally fine mesh is surrounded by a coarsening of the mesh in either direction (the

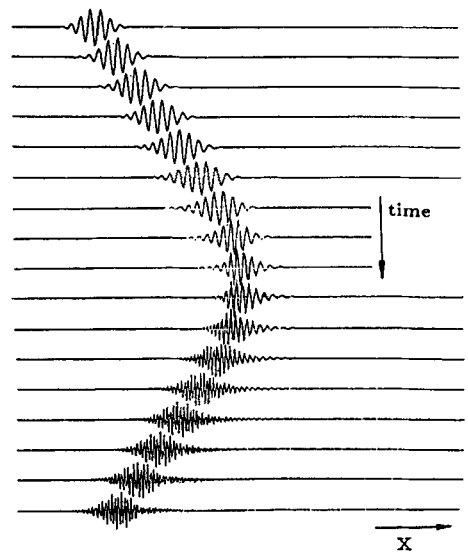

Figure 2. Reflection of a numerical wave packet (the numerical analogue of an elementary mass particle) by the potential gradient shown in Figure 3

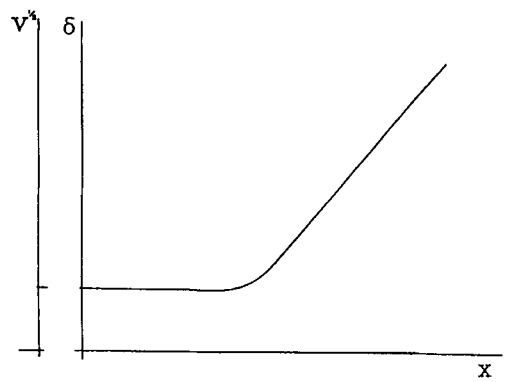

Figure 3. Space dependence of the mesh size (and of the resulting potential) used to create the reflection of a wave packet shown in Figure 2

corresponding geometry is sometimes referred to as a 'grid well'). The same wave group may then undergo successive internal reflections and remain trapped inside the computing domain.[11,13] An illustration of this is given by the experiment whose results are shown in Figure 4. This example of a monochromatic solution trapped in a grid well will be of interest to us later on: it will be found that certain properties of its solutions bear a striking resemblance to those of the quantum mechanics harmonic oscillator.

6. FOURIER TRANSFORMS AND SCATTERING

The analogy of the behaviour of numerical wave packets with that of particles in classical mechanics described in the preceding section applies when mesh variations are continuous and slow. But a new class of phenomena takes place when this is no more the case, i.e. when abrupt variations in the mesh size are present: in the context of wave mechanics, the wave nature of matter (by de Broglie's relation) must be invoked to explain the process of scattering which occurs

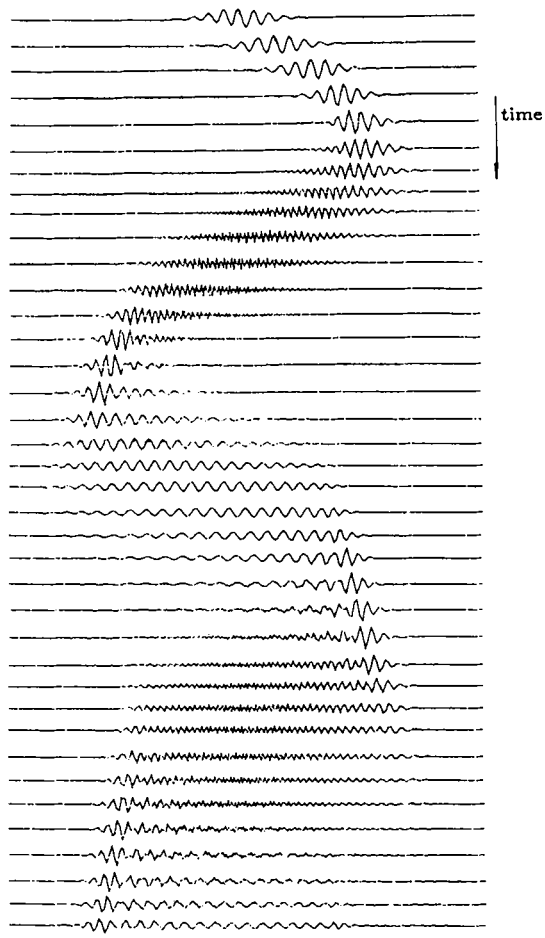

Figure 4. Multiple reflection of a wave packet in a 'grid well'. The mesh size is fine at the centre of the computing domain and increases geometrically with n in both directions toward the boundaries (from Reference 13). This creates an analogue of the mechanical harmonic oscillator. Note the gradual dispersion of the wave packet: this is explained in Section 7

when elementary particles pass across a step change in the potential. Likewise, the harmonic nature of numerical wave packets must be taken into account (which is done by using Fourier transforms) in the analogous situations which occur in computing domains. It will be useful, to set the stage for further developments, to briefly review those known results in the context of numerical wave propagation, underlining their similarity with those of quantum mechanics where applicable.

The time Fourier transform of a function $v(t)$ which belongs to a Hilbert space is defined as

$$\hat{v}(\omega) = \int_{-\infty}^{\infty} v(t) e^{-i\omega t} dt. \tag{25}$$

It is easily shown that if $\{u_n\}$ is a solution of (1) with δ constant, then it may be expressed as the sum of two modes of solution whose transforms satisfy the recurrence equations[10]

$$\left[\frac{\hat{u}_{n+1}(\omega)}{\hat{u}_n(\omega)}\right]_+ = \hat{E}_+(\omega) = -i\left(\frac{\omega\delta}{c}\right) + \left[1 - \left(\frac{\omega\delta}{c}\right)^2\right]^{1/2}, \tag{26}$$

$$\left[\frac{\hat{u}_{n+1}(\omega)}{\hat{u}_n(\omega)}\right]_- = \hat{E}_-(\omega) = -i\left(\frac{\omega\delta}{c}\right) - \left[1 - \left(\frac{\omega\delta}{c}\right)^2\right]^{1/2}. \tag{27}$$

When $|\omega|$ does not exceed the cut-off frequency ω_c, then $|\hat{E}_+(\omega)| = |\hat{E}_-(\omega)| = 1$, and (26), (27) describe waves which are harmonic in space as well as in time. The first is right-going, the second left-going, as described by their respective group velocities (derived earlier: equation (9)).

When $|\omega|$ exceeds the cut-off frequency ω_c, then these relations become

$$\frac{\hat{u}_{n+1}(\omega)}{\hat{u}_n(\omega)} \equiv \hat{E}_\pm(\omega) = -i\left\{\left(\frac{\omega\delta}{c}\right) \mp \left[\left(\frac{\omega\delta}{c}\right)^2 - 1\right]^{1/2}\right\} = e^{-i(\pi/2)} \exp\left[\mp \cosh^{-1}\left(\frac{\omega\delta}{c}\right)\right], \tag{28}$$

such that

$$|\hat{E}_+(\omega)| < 1, \qquad |\hat{E}_-(\omega)| > 1. \tag{29}$$

The corresponding solutions are evanescent: they are harmonic in time but vary exponentially in space at a rate which increases with $|\omega| - \omega_c$ (Figure 5). The wave mass and energy flows associated with those solutions are zero. Their group velocity is imaginary. In quantum mechanics, evanescent solutions of Schrödinger's equation also occur. They exist inside potential walls where particles are, by classical mechanics' laws, forbidden to go, and they provide the explanation for the typically quantum mechanical phenomenon of tunnelling. Interestingly, one may conduct the same tunnelling experiments with numerical wave packets and observe analogous results (see Section 10 below, in particular Figures 14–16). Together with the analytical expression (28), those experiments will provide us with an additional point of reference for the development of the Schrödinger-like theory of numerical wave propagation that will be given below.

Time Fourier transforms are the appropriate tool for the description of scattering (or reflection): consider for instance a right-going monochromatic numerical wave on a uniform grid arriving from the left (where $\delta = \delta_L < |c/\omega|$) to a point of discontinuity beyond which the mesh is again uniform but of a different size ($\delta = \delta_R$). One of two things may happen: either partial reflection (also called scattering) when the potential beyond the discontinuity does not exceed the total energy of the incident solution (in the sense of Sections 4 and 5); or total reflection when this is not the case.

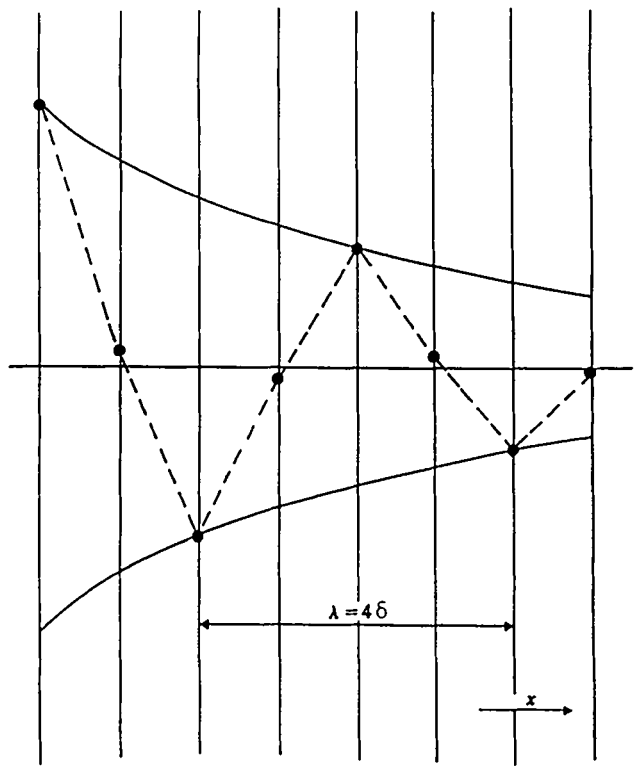

Figure 5. Evanescent numerical solution in a uniform grid (δ = constant, $\omega\delta > c$). These solutions are characterized by spatial oscillations of a wavelength equal to 4δ, modulated by a real exponential envelope.[10] Solutions of this type may be generated by applying a sinusoidal condition of the appropriate frequency at a boundary point. They are also formed inside potential walls during the process of tunnelling (see Section 10)

This process may be expressed by an amplitude reflection ratio[1,6,10]

$$\rho \equiv \frac{\hat{r}(\omega)}{\hat{s}(\omega)} = \frac{\left[1-\left(\frac{\omega\delta_L}{c}\right)^2\right]^{1/2} - \left[1-\left(\frac{\omega\delta_R}{c}\right)^2\right]^{1/2}}{\left[1-\left(\frac{\omega\delta_L}{c}\right)^2\right]^{1/2} + \left[1-\left(\frac{\omega\delta_R}{c}\right)^2\right]^{1/2}} = \frac{G_L(\omega) - G_R(\omega)}{G_L(\omega) + G_R(\omega)}, \tag{30}$$

where $\hat{s}(\omega)$ and $\hat{r}(\omega)$ are the Fourier transforms of the incident and reflected solutions at the point of discontinuity, and G_L and G_R are the group velocities in the corresponding half-spaces. This is similar to a well known result in the theory of transmission lines, expressing signal reflection at the junction of two lines of different characteristic impedance (see e.g. Reference 20, p. 113). What is more relevant to us is the fact that the same relation applies to the wavefunction of atomic particles, describing scattering at points of discontinuity of the potential (see Reference 19, p. 81).

While r and s correspond to the same frequency ω, their wave numbers are different: they are the two roots of the dispersion relation (7) solved for ξ, i.e.

$$|\xi_r| = \pi/\delta_L - |\xi_s|. \tag{31}$$

This jump in wave number during scattering is clearly visible in the numerical example illustrated in Figure 6.

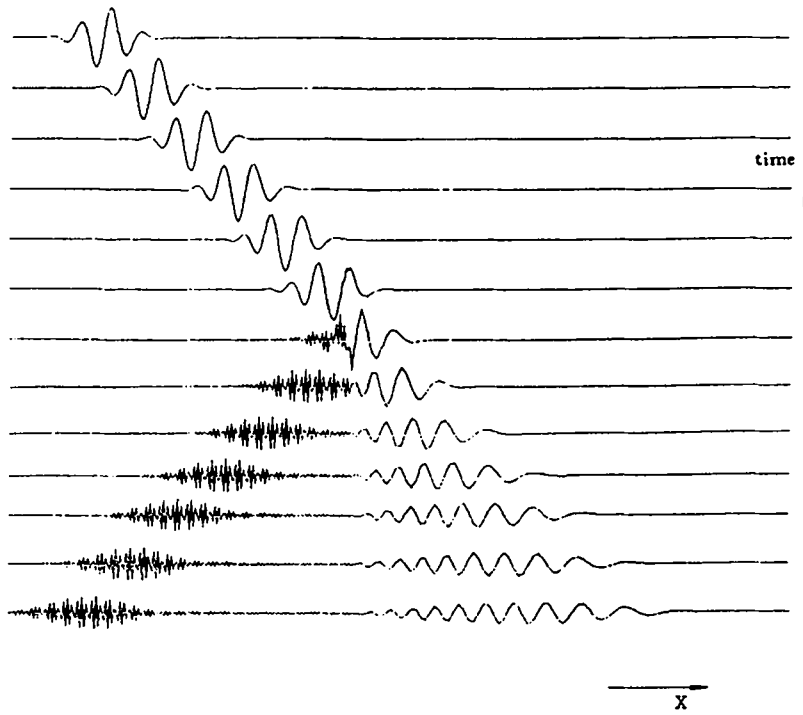

Figure 6. Scattering of a numerical wave packet at the interface between two uniform grids of different mesh sizes

7. STANDING WAVES

Standing waves will turn out to be of significant theoretical interest. The kind of standing waves we shall be concerned with are those which occur where left-going and right-going solutions exist simultaneously, i.e. are superimposed.

A first example of this occurs in grid wells: if the experiment illustrated in Figure 4 is allowed to continue for a long time, then the wave mass which was initially concentrated in a packet of small support in the computational space will be gradually dispersed and will eventually approach a stationary distribution. The reason for this is as follows: If η is an approximate measure of the width of the initial wave packet, then, by the bandwidth theorem, its width in ξ Fourier space is of order $1/\eta$ (i.e. finite). The mass associated with each wave number in this band travels at its own group velocity. Since $\partial G/\partial \xi \neq 0$, this causes the packet to spread (or disperse). As $t \to \infty$, it will have distributed itself over the entire region over which waves of the corresponding frequency may exist, i.e. where

$$\left|\frac{\omega\delta}{c}\right| \leqslant 1 \quad \text{or} \quad \delta \leqslant \delta_c = \left|\frac{c}{\omega}\right|. \tag{32}$$

This may be observed in Figure 7.

A second instance of stationary waves is obtained by applying a steady sinusoidal condition at the upwind boundary of a computing domain D in which total or partial reflection is taking place. Letting

$$u_0(t) = 2s_0(t) - u_1(t), \qquad s_0(t) = e^{i\omega t} \tag{33}$$

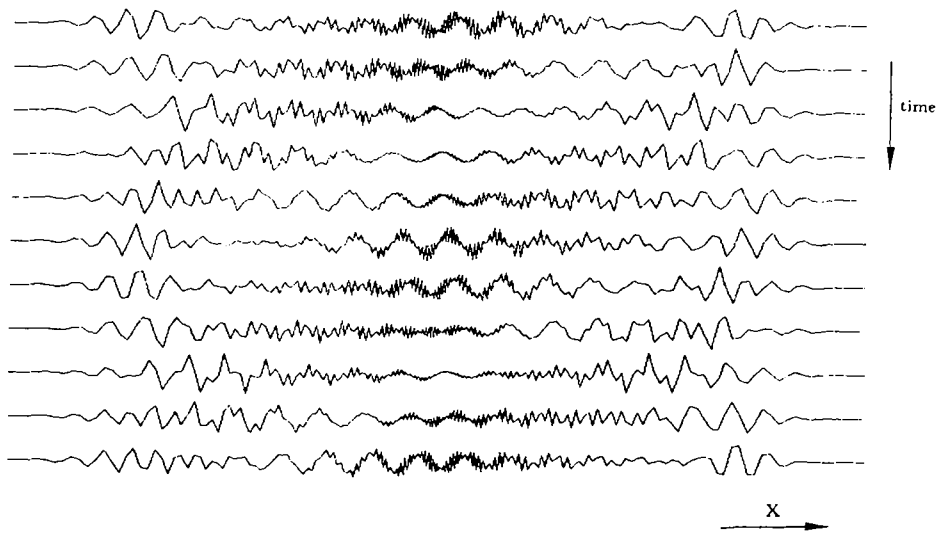

Figure 7. (Almost) monochromatic standing wave obtained by letting the experiment of Figure 4 run for a long time (the time Fourier spectrum in any given point is concentrated near the single frequency ω of the original wave packet)

(where u_0 and u_1 are the numerical values at the boundary and at the first point downwind) results, to within negligible terms, in a right-going solution of frequency ω and amplitude equal to 1, and in the absorption in $x = 0$ of the left-going (reflected) solution returning from D.[9, 21] By contrast with the preceding example, the standing wave obtained in this case is (after disappearance of an initial transient) purely monochromatic (Figure 8).

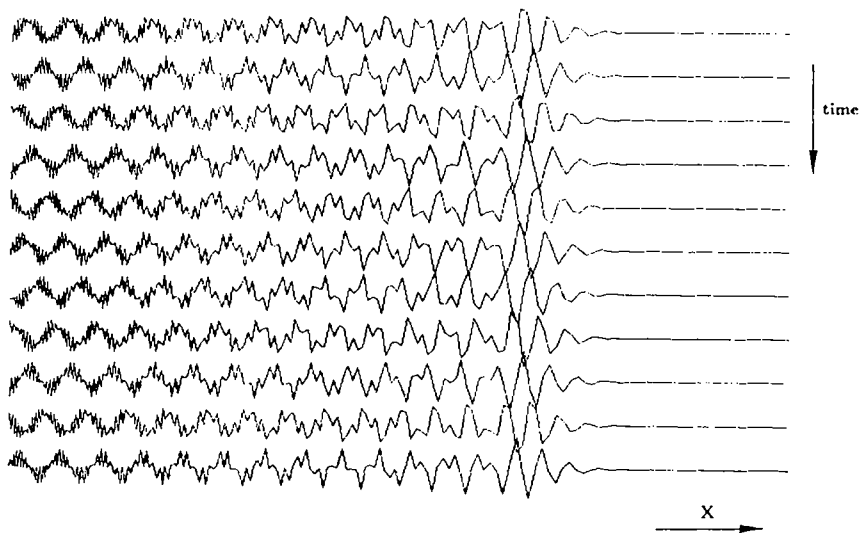

Figure 8. Monochromatic standing wave obtained by applying a sinusoidal condition at the upwind boundary (to the left) of a computing domain in which a stretching of the mesh ($\delta_{n+1}/\delta_n = 1{\cdot}02$) creates internal reflection. These curves consist of a long-wavelength, right-going solution which is superimposed on one that is reflected, short-wavelength and left-going

Standing waves imply that there is a zero net mass flow through any given point. Whence (see Section 3) (equality of left-going and right-going flows)

$$|u_+(x,t)|^2 = |u_-(x,t)|^2 \tag{34}$$

and obviously (steady state)

$$\frac{\partial}{\partial t}|u_+(x,t)|^2 = \frac{\partial}{\partial t}|u_-(x,t)|^2 = 0. \tag{35}$$

By the conservation law (11) this implies

$$\frac{\partial}{\partial x}(G_+|u_+|^2) = \frac{\partial}{\partial x}(G_-|u_-|^2) = 0. \tag{36}$$

The same relation should also apply to the sum of u_+ and u_-, but in a mean sense only: phase interference phenomena (invoking the internal oscillatory nature of the wave packets) will come into play. This question is examined next.

8. NEW EXPERIMENTAL RESULTS

It may be argued that the analogies with physics encountered so far have invoked not much more than de Broglie's wave mechanics, providing an explanation of the fact that the wave/particle duality of matter and the wave/wave packet duality of monochromatic numerical solutions share similar mathematics.

But we will now examine situations where more specific analogies with quantum mechanics are revealed: an instance of this is in the following results, which were obtained (unexpectedly) in numerical experiments aimed at verifying that (36) indeed applies to the distribution of $|u(x,t)|^2$ in standing monochromatic waves. To conduct such experiments, the oscillatory time dependence of u was eliminated by computing time averages

$$\langle u^2(x)\rangle = \frac{1}{t_A}\int_0^{t_A} u^2(x,t)\,dt, \tag{37}$$

where t_A is reasonably larger than the period τ:

$$t_A \gg \tau = 2\pi/\omega. \tag{38}$$

In the absence of phase interference phenomena (i.e. if the 'particle' aspect of the waves were sufficient to describe the situation), the experimental data would satisfy

$$\frac{\partial}{\partial x}[G(\omega,x)\langle u^2(x)\rangle] = 0 \quad \text{or} \quad \langle u^2(x)\rangle \sim \frac{1}{G(\omega,x)}. \tag{39}$$

The results of a first numerical example, in which the average steady state distribution $\langle u^2\rangle$ in a grid well has been computed, is given in Figure 9: upon the smooth distribution described by (39) are superimposed spatial oscillations which have a wavelength clearly related to δ, and which must be related to the wave nature of u_+ and u_-. The results of a second example (Figure 10), that of $\langle u^2\rangle$ for the standing wave of Figure 8, display similar spatial oscillations.

While one could possibly search for an analytic description of this by invoking simple principles of elementary wave superposition, the striking resemblance of those oscillations to those of the wavefunction in quantum mechanics has been noted. For instance, the experimetal data shown in Figure 9 are strongly reminiscent of the Hermite functions which are precisely the

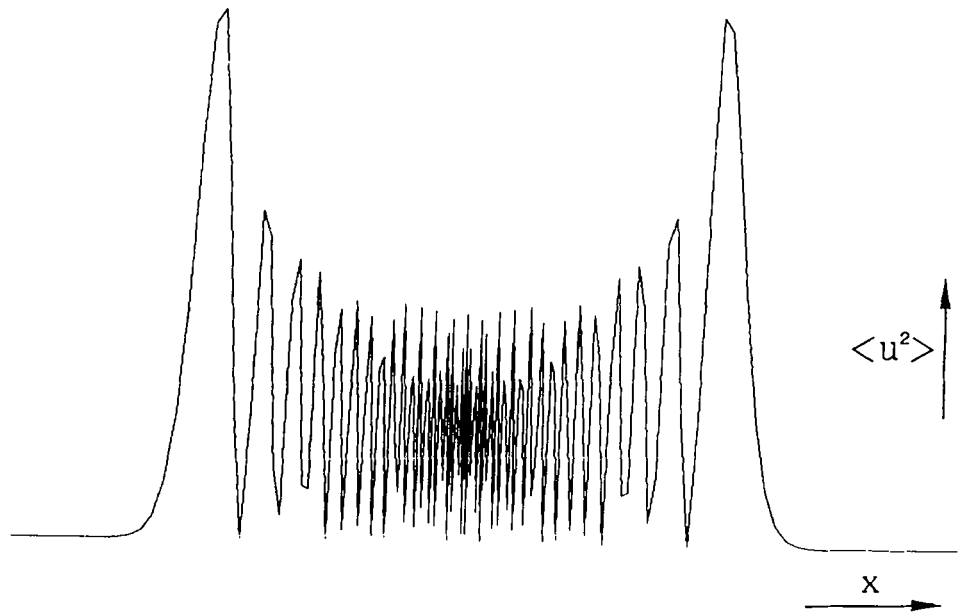

Figure 9. Time average of the square of the numerical standing wave illustrated in Figures 4–7 obtained by placing a numerical wave packet in a grid well, thus creating a wave mechanics counterpart of the harmonic oscillator. The spatial oscillations that may be observed are evidently similar to those of the corresponding wavefunction in quantum mechanics

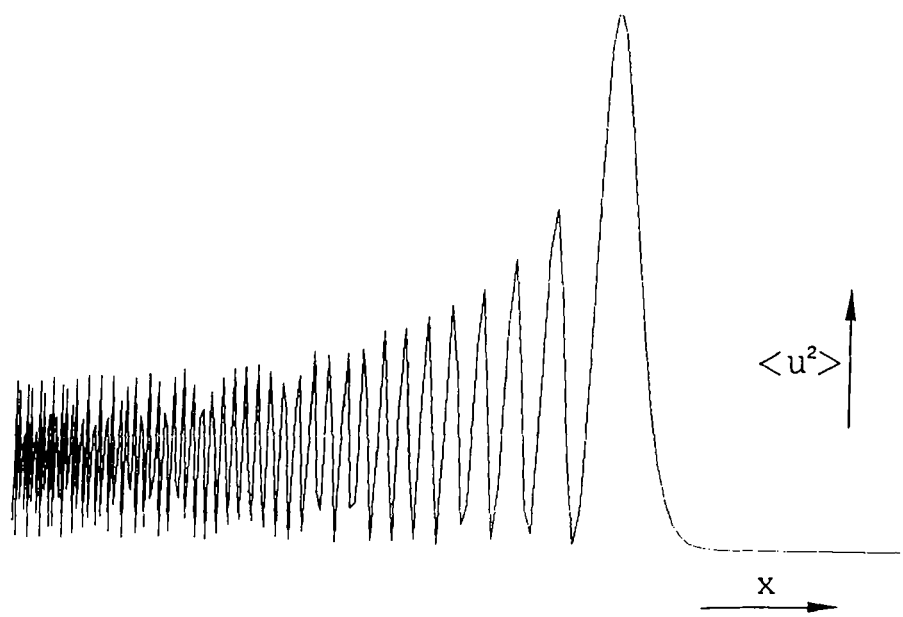

Figure 10. Time average of the square of the monochromatic standing wave shown in Figure 8

solutions of Schrödinger's equation for the linear harmonic oscillator that is the mechanical analogue of this case (see e.g. Reference 22, p. 502). This has suggested that a more fundamental (closer to quantum mechanics) theoretical explanation could be found. Showing that this is indeed the case will be our next objective.

9. INTRODUCTION TO A NEW FORMALISM (OR THEORY)

Schrödinger's equation of quantum mechanics gives a direct relationship between the classical mechanics Hamiltonian of a mass particle and its associated wavefunction (also described by de Broglie's relation). The principal result of this paper will be to show that a similar equation may be derived in the case of numerical wave propagation, establishing a direct relationship between a Hamiltonian coming from the mechanical description of wave packets derived earlier and a wavefunction related to the original wave by a simple, unitary transformation.

It will be useful to summarize the experimental and theoretical facts against which the new theory will have to be validated:

1. It should agree with the known results in (numerical) wave propagation reviewed in Section 3, in particular with the conservation law (11) which describes the dynamics of the envelope of numerical solutions when $|\omega| < \omega_c$.
2. The conservation law (11) does not apply when $|\omega| > \omega_c$, but evanescent solutions exist in that case. They are known analytically when δ = constant (equation (28)). It will be found that they are indeed contained in the new theory, explaining the similarity between numerical and quantum mechanics tunnelling.
3. The new theory should account analytically for the spatial oscillations in standing waves described in the preceding section.

In Schrödinger's theory, to a particle of momentum P and total energy E is associated a wavefunction of the form (see e.g. Reference 18 or 22, or Reference 19, Chapters I and II)

$$\psi(x, t) = \varepsilon(x, t)\exp\left[-\frac{2\pi i}{h}\left(Et - \int^x P\,dx \right)\right], \tag{40a}$$

where h is Planck's constant. This wavefunction satisfies the equation obtained by replacing in the corresponding Hamiltonian

$$H \equiv T(x, P) + V(x) = E$$

the momentum P and total energy E by the operators

$$P \sim \frac{h}{2\pi i}\frac{\partial}{\partial x}, \tag{41a}$$

$$E \sim -\frac{h}{2\pi i}\frac{\partial}{\partial t}. \tag{41b}$$

The frequency of ψ is related to the energy by de Broglie's relation

$$\omega = 2\pi\nu = 2\pi E/h, \tag{40b}$$

and the function

$$-Et + \int^x P\,dx \tag{40c}$$

in its imaginary exponent is Hamilton's principal function, which plays an important role in the description of a mass particle's dynamics (the Hamilton–Jacobi theory—see e.g. Reference 17).

A basic assumption shall be that if numerical wave propagation and quantum mechanics both describe objects which may be represented by wave packets, with the additional constraint that some of the variables can change by discrete steps (or quanta) only, then it is probable that similar mathematics (including those aspects of 'classical' quantum mechanics which are somewhat pragmatic) will apply to both. But there are essential differences, resulting from the fact that it is spatial position which is discretized (or quantized) in the present case, and energy levels in quantum mechanics. As the following will show, a coherent theory can be developed that takes these differences into account.

We begin by assuming that the spatial oscillations observed in Section 8 are those of a wavefunction similar to (40a) in Schrödinger's theory, viz.

$$W(x,t) = a(x,t)\exp\left[\,\mathrm{i}\left(\omega t - \int^{x} b\,\mathrm{d}x\right)\right], \tag{42}$$

where ω and b will be appropriately related to H and P. We shall then seek a set of operator relations which parallel (41). An implicit assumption in this expression is that W and u will have the same frequency ω: there was no reason to expect that it would be otherwise, and the subsequent analysis will verify that this *a priori* choice was indeed correct.

The important 'quantum' property of numerical wave propagation lies in the fact that space is discretized. This will mean, in particular, that derivatives with respect to x are to be replaced by their finite difference equivalent defined in (1), viz. (assuming a slow variation of δ)

$$\frac{\Delta v(x)}{\Delta x} = \frac{v(x+\delta) - v(x-\delta)}{2\delta}. \tag{43a}$$

In particular, the discrete derivative of an oscillatory function such as $\mathrm{e}^{\mathrm{i}\gamma x}$ will be

$$\frac{\Delta \mathrm{e}^{\mathrm{i}\gamma x}}{\Delta x} = \mathrm{i}\frac{\sin(\gamma\delta)}{\delta}\mathrm{e}^{\mathrm{i}\gamma x}. \tag{43b}$$

Note that the presence of an imaginary exponent in (42) creates two scales with respect to spatial variations. Indeed, it may be observed that with A and γ in the following expression both assumed to be slowly variable with respect to length scales of order δ, we shall have

$$\frac{\Delta}{\Delta x}(A\,\mathrm{e}^{\mathrm{i}\gamma x}) = \left(\frac{\mathrm{d}A}{\mathrm{d}x} + \mathrm{i}A\frac{\sin(\gamma\delta)}{\delta}\right)\mathrm{e}^{\mathrm{i}\gamma x}, \tag{43c}$$

since the difference between $\mathrm{d}A/\mathrm{d}x$ and $\Delta A/\Delta x$ is inconsequential while that between $\sin(\gamma\delta)/\delta$ and γ is not.

There is more than one Hamiltonian formulation that is consistent with the classical mechanics description of monochromatic waves derived earlier. The following (not necessarily unique) will result in a theory that is in agreement with the desiderata 1–3 set forth earlier. The wave kinetic energy is redefined as

$$T^* = G^2/2\bar{\delta}, \tag{44}$$

where $\bar{\delta}(x)$ is the dimensionless variable $\omega\delta(x)/c$ and the $*$ superscript defines the new variables. The corresponding wave momentum is obtained by the relation from classical mechanics

$$P = \frac{\partial T^*}{\partial(\mathrm{d}x/\mathrm{d}t)} = \frac{\partial T^*}{\partial G} = \frac{G}{\bar{\delta}}. \tag{45}$$

As noted in Section 5, these variables may be interpreted either as the specific variables of a continuous distribution $|u(x, t)|^2$ or as describing the configuration space of a single wave packet of unit mass.

The Hamiltonian expressed as a function of P and x will be

$$H = \frac{P\bar{\delta}(x)P}{2} + V^*(x) = c^2, \tag{46}$$

where the potential function V^* is

$$V^*(x) = c^2 - \frac{G^2(x)}{2\bar{\delta}(x)}. \tag{47}$$

(We note in passing that the dependence of both V^* and G upon x is only through the dimensionless number $\bar{\delta}(x)$, i.e. $V^*(x) = V^*(\bar{\delta}(x))$ and $G(x) = G(\bar{\delta}(x))$.) It may be verified that (other than for changes of definitions) the new variables are consistent with the classical mechanics formulation of Sections 4 and 5. Indeed, with x and G satisfying the 'classical' relations (24), we find

$$\frac{\partial H}{\partial P} = \bar{\delta}P = G = \frac{\mathrm{d}x}{\mathrm{d}t},$$

$$\frac{\partial H}{\partial x} = \left[\frac{P^2}{2} + \frac{c^2}{2}\left(\frac{1}{\bar{\delta}^2(x)} + 1\right)\right]\frac{\partial \bar{\delta}}{\partial x} = -\frac{\mathrm{d}P}{\mathrm{d}t}, \tag{48}$$

which are in the form of Hamilton's canonical equations. The total energy may in general be defined to within an arbitrary constant: its value c^2 in (46) is that which has been found (consistently with (44)) to result in the desired agreement with 1–3 listed at the beginning of this section.

As in Schrödinger's theory, we are to find equivalence rules that will replace H and P in (46) by differential (and, in the present case, difference) operators to produce an equation to be satisfied by W. If the operator equivalent of H applied to W is to be equal to the total energy multiplying W, then we shall have simply

$$\boxed{H \sim -\mathrm{i}\frac{c^2}{\omega}\frac{\partial}{\partial t}} \tag{49}$$

which is the first equivalence rule. The connection of Schrödinger's formalism with the Hamilton–Jacobi theory requires, as in (40a), that the imaginary exponent of the wavefunction be proportional to Hamilton's principal function (40c): to satisfy this requirement, the substitution rule for P must be of the form

$$P \sim \mathrm{i}\frac{c^2}{\omega}\frac{\partial}{\partial x}. \tag{50}$$

This, however, does not recognize the fact that space is discretized: spatial derivatives are to be interpreted as in (43) in the present context, and we must assume that the correct substitution rule

will be that which takes this into account, viz.

$$\boxed{P \sim \mathrm{i}\frac{c^2}{\omega}\frac{\Delta}{\Delta x}} \tag{51}$$

instead of (50). The subsequent analysis will show that this is indeed the appropriate assumption.

10. STEADY STATE MONOCHROMATIC WAVES

This case corresponds to solutions which are harmonic in time, with a stationary, space-dependent amplitude. They include, but are not restricted to, the standing waves described in Section 7: one-directional waves generated by a sustained sinusoidal condition at the upwind boundary of a semi-infinite domain are also 'steady state'.

We shall seek a wavefunction of the form

$$W(x,t) = a(x)\exp\left[\mathrm{i}\left(\omega t - \int^x b(x)\,\mathrm{d}x\right)\right] = w(x)\mathrm{e}^{\mathrm{i}\omega t}, \tag{52}$$

where

$$w(x) = a(x)\exp\left(-\mathrm{i}\int^x b(x)\,\mathrm{d}x\right) \tag{53}$$

depends on x alone.

This wavefunction is to be the solution of the equation derived from the Hamiltonian with the substitution rule (51), and which shall hold a central place in the subsequent theory:

$$\boxed{\frac{1}{2}\left(\frac{c^2}{\omega}\right)^2 \frac{\Delta}{\Delta x}\left(\bar{\delta}\frac{\Delta}{\Delta x}\right)w(x) + [c^2 - V^*(x)]w(x) = 0.} \tag{54}$$

This *new equation* has of course evident similarities with Schrödinger's equation, but it differs in particular in that it contains finite differences instead of derivatives. Another noteworthy difference is that $\bar{\delta}$ (which plays a role in the new theory somewhat similar to the role of Planck's constant in quantum mechanics) is not a constant and will in general be a function of x.

Examining the nature of solutions to (54) is best done separately for the cases where $V < H$ and $V > H$.

(*a*) $V < H$ (*or* $|\bar{\delta}| < 1$)

Equation (54) may then be rewritten as

$$\left(\frac{c^2}{\omega}\right)^2 \left(\bar{\delta}\frac{\Delta}{\Delta x}\right)^2 w(x) + G^2(x)w(x) = 0. \tag{55}$$

Inserting (53) in this equation results in a complex expression which may be decomposed into its

real and imaginary parts, viz.

real part

$$\frac{\Delta}{\Delta x}\left(\delta c\frac{\Delta}{\Delta x}\right)a(x) - a\left[\delta c\left(\frac{\sin(b\delta)}{\delta}\right)^2 - \frac{G^2}{\delta c}\right] = 0, \tag{56}$$

imaginary part

$$\frac{\Delta}{\Delta x}[ac\sin(b\delta)] + \frac{\Delta a}{\Delta x}c\sin(b\delta) = 0. \tag{57}$$

An approximate solution may be found in closed analytic form by using a finite difference analogue of the WKB (Wentzel, Kramers and Brillouin) method, which was developed for this very purpose in the context of the classical Schrödinger equation (see Reference 23, pp. 1092 *et seq.*). We assume that the leading term of equation (56) may be neglected—which is justified by the facts that this leading term is of a higher order in δ and that $a(x)$ has been assumed to vary slowly with respect to x. This leaves

$$\sin(b\delta)^2 - \left(\frac{G}{c}\right)^2 = 0 \quad \text{or} \quad \sin(b\delta) = \pm\left|\frac{G}{c}\right|, \tag{58}$$

with the two signs corresponding to right-going and left-going waves respectively; and (57) becomes

$$\frac{\mathrm{d}}{\mathrm{d}x}[G(x)a^2] = 0, \tag{59}$$

where, since G and a vary slowly with respect to x, the operator $\Delta/\Delta x$ has been replaced by $\mathrm{d}/\mathrm{d}x$ (see the remark above which contains equation (43c)). We note that (59) is precisely the expression of the conservation law (11) in the stationary case ($\partial\alpha/\partial t = 0$). Therefore (guided by the analogy with classical quantum mechanics) we shall take

$$a(x) = \alpha(x) \tag{60}$$

which is indeed a solution of (59). The solution of (58) for b has two possible roots of each sign of the equation. The one that produces a coherent relation between W and u is

$$b_\pm = \frac{1}{\delta}\left(\pi \mp \sin^{-1}\left|\frac{G}{c}\right|\right). \tag{61}$$

This choice of solutions for a and b results in

$$w_\pm(x) = \alpha(x)\exp\left[-\mathrm{i}\int\left(\pi \mp \sin^{-1}\left|\frac{G}{c}\right|\right)\frac{\mathrm{d}x}{\delta}\right]$$

and

$$W_\pm(x,t) = \alpha(x)\mathrm{e}^{\mathrm{i}\omega t}\exp\left[-\mathrm{i}\int\left(\pi \mp \sin^{-1}\left|\frac{G}{c}\right|\right)\frac{\mathrm{d}x}{\delta}\right] \tag{62}$$

which will apply separately to the right-going (+) and left-going (−) components of u. Returning to the discrete expression of these waves reveals the interestingly simple form

$$W_{\pm,n}(t) = (-1)^n\alpha_n\mathrm{e}^{\mathrm{i}\omega t}\exp\left(\pm\mathrm{i}n\sin^{-1}\left|\frac{G}{c}\right|\right). \tag{63}$$

It may be verified that the simple unitary (i.e. amplitude-preserving) relation

$$W_{\pm}(x,t) = \exp\left(-\mathrm{i} \int \frac{\pi \, \mathrm{d}x}{2\delta} \right) u_{\pm}(x,t) \tag{64}$$

holds between W and u. The discrete form of this relation is

$$W_{\pm,n} = (-\mathrm{i})^n u_{\pm,n}. \tag{65}$$

Needless to say, realizing that the choices (60) and (61) for a and b resulted in such a simple relationship between W and u was a determining factor in making those choices. Moreover, it may be verified that the group velocity of W (which may be derived from the imaginary exponent in (62) is equal to that of u, a result of significant theoretical importance.

The distribution of W^2 is found to be equal to that of u^2:

$$|W_{\pm}(x,t)|^2 = |u_{\pm}(x,t)|^2. \tag{66}$$

This quantity is interpreted in quantum mechanics as a probability distribution. A similar viewpoint may be adopted here, interpreting $|u(x,t)|^2$ as describing the configuration space of a single wave packet of unit wave mass. The normalizing relation

$$|W_{\pm}(x,t)|^2 = |u_{\pm}(x,t)|^2 = 1 \tag{66a}$$

then applies to both u and W.

When a left-going wave (u_-) and right-going wave (u_+) of the same frequency ω are added, then the same will apply to their respective wavefunctions. In the particular case of standing waves corresponding to the superposition of such left-going and right-going waves of equal amplitude (those of Sections 7 and 8), then this will result in

$$\begin{aligned} u_+ + u_- &= \exp\left(+\mathrm{i} \int \frac{\pi \, \mathrm{d}x}{2\delta} \right)(W_+ + W_-) \\ &= \alpha(x) \mathrm{e}^{\mathrm{i}\omega t} \exp\left(-\mathrm{i} \int \frac{\pi \, \mathrm{d}x}{2\delta} \right) 2\cos\left(\int^x \sin^{-1} \left| \frac{G}{c} \right| \frac{\mathrm{d}x}{\delta} \right). \end{aligned} \tag{67}$$

When the averaged square of this function is computed, then the term

$$\left[\mathrm{e}^{\mathrm{i}\omega t} \exp\left(-\mathrm{i} \int \frac{\pi \, \mathrm{d}x}{2\delta} \right) \right]^2 \tag{68}$$

averages to a constant. This leaves

$$\begin{aligned} \langle (u_+ + u_-)^2 \rangle = \langle (W_+ + W_-)^2 \rangle &= \text{constant} \times \alpha^2(x) \cos^2\left(\int^x \sin^{-1} \left| \frac{G}{c} \right| \frac{\mathrm{d}x}{\delta} \right) \\ &= \text{constant} \times \alpha^2(x) \cos^2\left(n \sin^{-1} \left| \frac{G}{c} \right| \right), \end{aligned} \tag{69}$$

containing a locally sinusoidal term of wavelength half (because of the squaring) that of the corresponding term in the wavefunctions W_+ and W_-, viz.

$$\lambda = \frac{2\pi\delta}{\sin^{-1} |G/c|}. \tag{70}$$

Verification (i). It is found (with an agreement of better than 1%, which is the accuracy afforded by the computation) that this is the wavelength of the spatial oscillations observed in the time-averaging experiments of Section 8. See Figure 11 for an illustration.

This was a crucial test. Indeed, one can develop a similar Schrödinger-like theory with the continuous operator (50) instead of the discrete (51). But, in addition to being inconsistent with the present circumstances, the wavelength of the corresponding wavefunction does not agree with this experimental data.

Verification (ii). When the oscillations of $\langle u^2 \rangle$ are removed by a spatial averaging, then it is found that the spatially averaged $\langle u^2 \rangle$ verifies the conservation law (11).

(*Note.* Earlier work reported in Reference 13 was concerned with the development of a theory to account for the behaviour of spurious solutions that remain trapped by internal reflection inside the computing domain of certain large-scale aerodynamic calculations. It is in numerical experiments aimed at verifying the conservation law (11) for such solutions that the spatial oscillations of Section 8 were first observed, and it was found that space averaging has to be introduced to be able to verify conservation.)

By contrast, the time-averaged square of a sustained (i.e. also stationary) one-directional wave results in

$$\langle u^2(x) \rangle = \langle W^2(x) \rangle = \text{constant} \times \alpha^2(x) \tag{69}$$

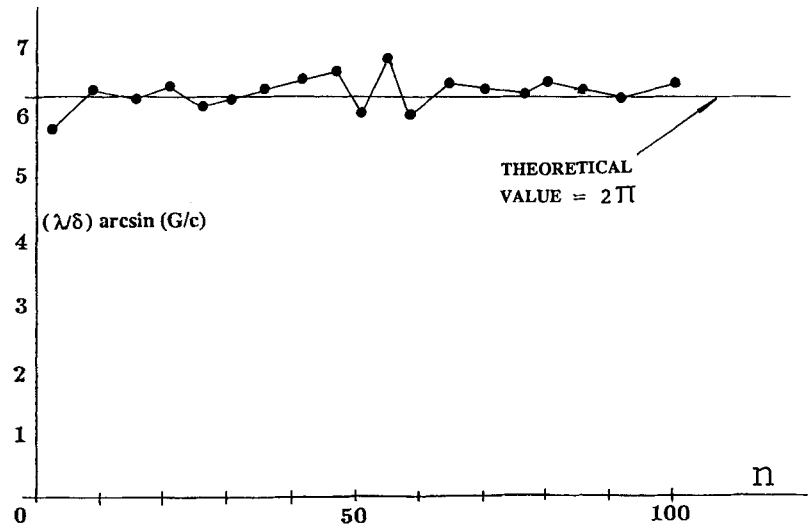

Figure 11. Wavelength of the oscillations of the experiment of Figures 4–9 (normalized by the factor $\sin^{-1}(G/c)/\delta$) compared with the value 2π predicted by the theory. These values were recorded by the computer program by quadratic interpolation between points near the peaks of Figure 9. Individual values of λ agree with the theoretical value to within a few %, and the agreement of the mean value of λ for this experiment is better than a fraction of 1%. Values of λ/δ, and G/c vary from 4·2 and 0·98 respectively near the centre of the domain to 10·2 and 0·51 towards its ends

which does not display spatial oscillations. An illustration and verification of this will be given later (in Figure 16).

(*b*) $V > H$ (*or* $|\bar{\delta}| > 1$

We may rewrite equation (54) as

$$\boxed{\left(\delta \frac{\Delta}{\Delta x}\right)^2 w(x) - (\bar{\delta}^2 - 1)w(x) = 0} \tag{71}$$

(where $\bar{\delta}^2 - 1 > 0$) which admits solutions of the form (53) but with a complex exponent. When δ is constant, then this equation may be rewritten as

$$\left[\left(\frac{\Delta}{\Delta x}\right)^2 - \frac{1}{\delta^2}(\bar{\delta}^2 - 1)\right] w(x) = \left(\frac{\Delta}{\Delta x} + \frac{1}{\delta}(\bar{\delta}^2 - 1)^{1/2}\right)\left(\frac{\Delta}{\Delta x} - \frac{1}{\delta}(\bar{\delta}^2 - 1)^{1/2}\right) w(x) = 0 \tag{72}$$

which admits as solutions (having taken (43) into account)

$$w_{\pm}(x) = e^{-i\pi x/\delta} \exp\left(\mp \frac{x}{\delta} \cosh^{-1}(\bar{\delta})\right) \quad \text{or} \quad w_{\pm,n} = (-1)^n \exp[\mp n \cosh^{-1}(\bar{\delta})], \tag{73}$$

and we obtain

$$W_{\pm}(x,t) = e^{i\omega t} e^{-i\pi x/\delta} \exp\left(\pm \frac{x}{\delta} \cosh^{-1}(\bar{\delta})\right) \quad \text{or}$$

$$W_{\pm,n}(t) = (-1)^n e^{i\omega t} \exp[\mp n \cosh^{-1}(\bar{\delta})] \tag{74}$$

Verification (*iii*). There is a perfect analytical identity between the expression of $W(x, t)$ in (74) and—by the unitary transformation (65)—the analytic expression of evanescent solutions obtained in closed form by simple Fourier analysis (Section 6, in particular equation (28)).

Verification (*iv*). Stationary evanescent solutions generally occur as one-directional (as opposed to the superposition of a right-going and left-going wave) in the proximity of boundaries from where they originate. Their averaged square

$$\langle u_{\pm}^2 \rangle = \langle w_{\pm}^2 \rangle = \text{constant} \times \exp\left(\mp 2 \frac{x}{\delta} \cosh^{-1}(\bar{\delta})\right) \tag{75}$$

then varies exponentially with distance, without spatial oscillations. The experimental data shown in Figures 13 and 16 verify that this is indeed the case.

These results explain numerical tunnelling in every respect, just as the corresponding theory does in quantum physics. This is illustrated in the following experiments: while the wave packet (or particle) shown in Figure 14 is in contact with the potential wall, it generates in that wall (where $V > H$ or $\bar{\delta} > 1$) an evanescent solution which lasts for the duration of the contact. This evanescent solution contains wave mass: if the wall were of infinite thickness, then this wave mass would return entirely with the reflected wave packet toward the left. But with a wall of finite

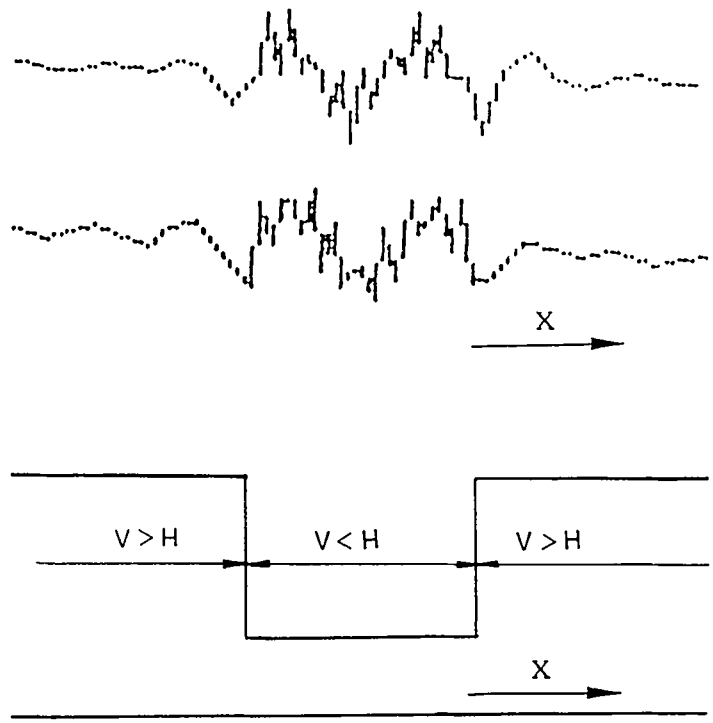

Figure 12. Standing monochromatic wave obtained by introducing a wave packet in a square potential well

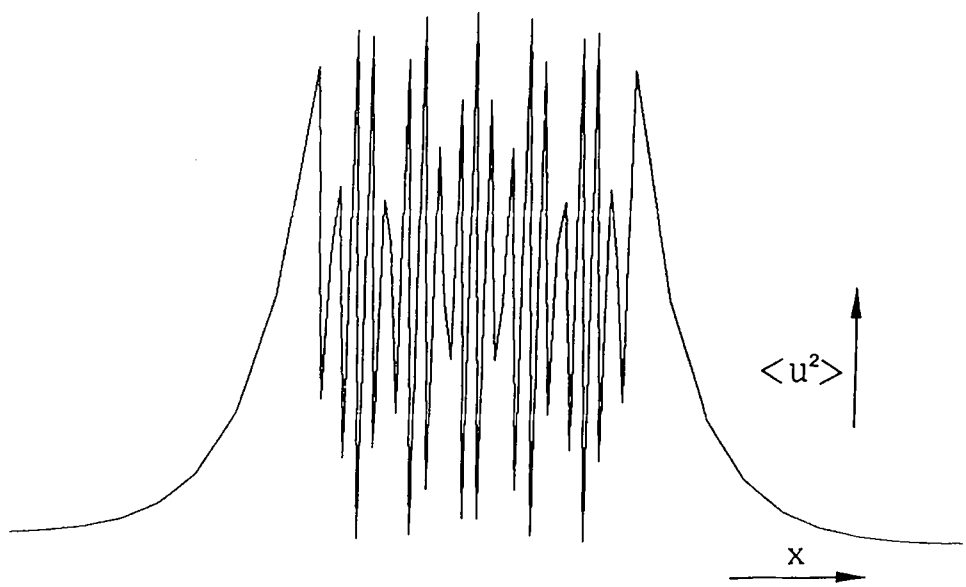

Figure 13. $\langle u^2(x) \rangle$ recorded in the numerical experiment illustrated in the preceding figure. As predicted by the theory, $\langle u^2 \rangle$ decays exponentially with distance (without spatial oscillations) outside the well where $V > H$. This rate of exponential decay is described by equation (75)

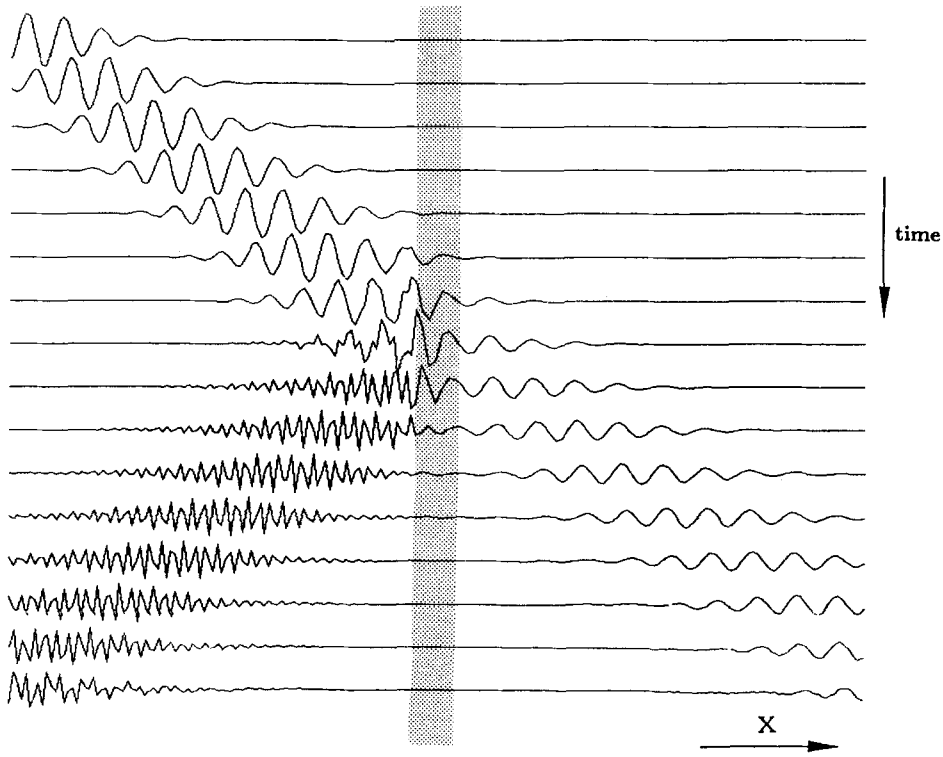

Figure 14. Tunnelling experiment with a single wave packet. The grid is piecewise constant, with $V < H$ in the white area and $V > H$ in the shaded area (creating a potential wall)

thickness some of that mass, i.e. that contained in the tail of the evanescent solution which would have extended beyond the end of the wall, escapes to the right and does not return, whence tunnelling. The same experiment is repeated in Figure 15 with a sustained sinusoidal wave of the same frequency (the equivalent of a beam of particles). While recordings of $\langle u^2 \rangle$ for the single particle show some interesting phenomena (not shown here), those of $\langle u^2 \rangle$ for the sustained sinusoidal wave display more vividly the properties of the wavefunction predicted by the tunnelling theory (Figure 16).

11. NON-STEADY STATE MONOCHROMATIC WAVES

Substituting (49) for H as well as (51) for P into (46) considered as an operator on W results in the equation

$$\boxed{\frac{1}{2}\left(\frac{c^2}{\omega}\right)^2 \frac{\Delta}{\Delta x}\left(\bar{\delta}\frac{\Delta}{\Delta x}\right) W(x,t) - V^*(x)\, W(x,t) = \mathrm{i}\frac{c^2}{\omega}\frac{\partial W(x,t)}{\partial t}} \tag{76}$$

which is, in the *new theory*, the counterpart of the time-dependent Schrödinger equation. Inserting (42) as a trial solution results as before in a complex equation, the real part of which is identical to

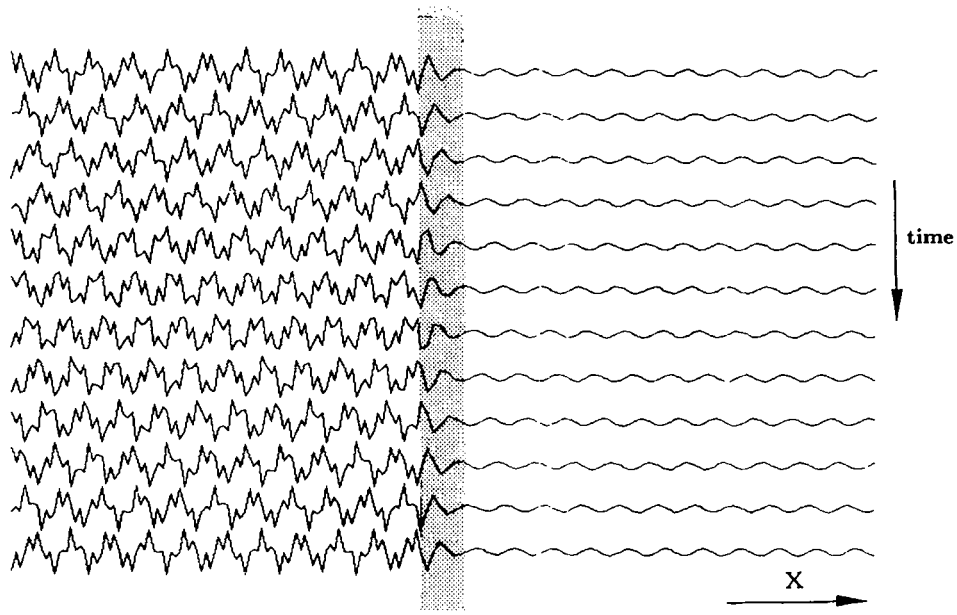

Figure 15. Repeat of the same tunnelling experiment with a continuous sinusoidal wave coming from the left (the analogue of a beam of physical particles). It may be observed that the wave inside the wall has a wavelength of 4δ, i.e. is indeed an evanescent solution (cf. Figure 5)

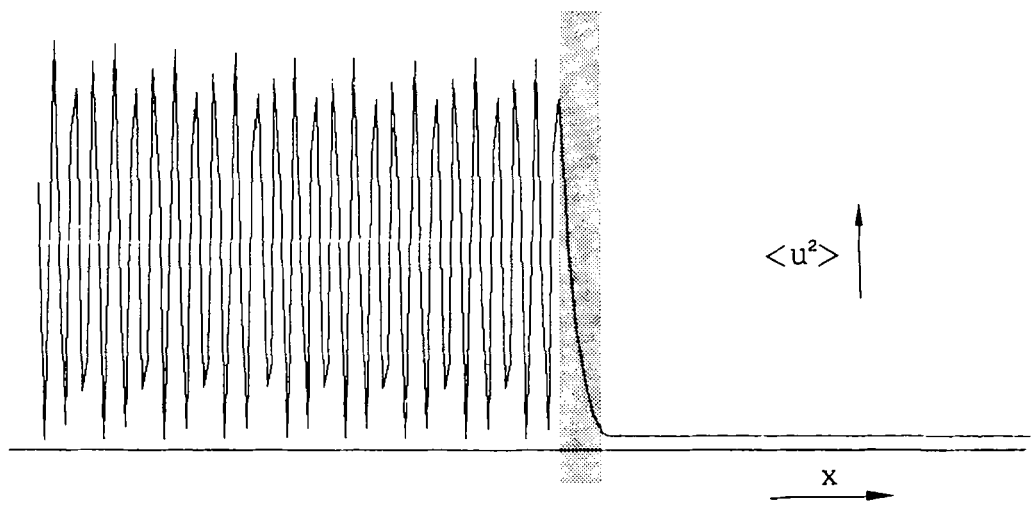

Figure 16. $\langle u^2(x) \rangle$ recorded in the tunnelling experiment illustrated in the preceding figure. One may observe. (a) spatial oscillations in $\langle u^2 \rangle$ to the left of the wall, similar to those of Figures 9 and 10, created by the superposition of the wavefunctions of the incident and reflected sustained waves; (b) exponential decay of $\langle u^2 \rangle$ inside the wall where the wave is evanescent (per equation (75)); (c) a space-independent $\langle u^2 \rangle$ to the right of the wall (per equation (69)) where there is only a sustained one-directional wave, that which has tunnelled across the wall

(56) (when $V < H$) while the imaginary part becomes

$$\frac{\Delta}{\Delta x}[ac\sin(b\delta)] + \frac{\Delta a}{\Delta x}(\sin(b\delta) = -2\frac{\partial a}{\partial t}. \tag{77}$$

The value of b is again given, within the WKB approximation, by (61), and equation (77) becomes

$$\frac{\partial a^2}{\partial t} + \frac{\partial}{\partial x}[G(x)a^2] = 0, \tag{78}$$

where, as before (and with the same justification), finite differences with respect to x have been replaced by the usual derivatives. Interestingly, this equation is precisely the conservation law (11), and

$$a(x, t) = \alpha(x, t) \tag{79}$$

is again an acceptable solution. We then obtain

$$W_{\pm}(x, t) = \alpha_{\pm}(x, t)e^{i\omega t}\exp\left[-i\int\left(\pi \mp \sin^{-1}\left|\frac{G}{c}\right|\right)\frac{dx}{\delta}\right] \tag{80}$$

or, in discrete form,

$$W_{\pm,n}(t) = (-1)^n\alpha_{\pm,n}(t)\exp\left(\pm i n \sin^{-1}\left|\frac{G}{c}\right|\right) \tag{81}$$

which is identical to (62) except for the time dependence of α. Moreover, the simple relation (64), (65) between W and u continues to hold in this non-steady case. This is consistent with the fact that W and u have the same group velocity, as has been noted in the preceding section.

12. CLOSING COMMENTS

We have shown that certain properties of numerical wave propagation resemble closely those of quantum mechanics, and that they may be described by a formalism akin to Schrödinger's theory. By contrast with the latter, the new theory describes 'large-scale' processes. In summary, to monochromatic waves which are solutions of (1) one may (for non-steady as well as steady problems) associate a wavefunction which satisfies a Schrödinger-like equation. This new equation is derived from a Hamiltonian which describes the dynamics of those monochromatic solutions, with substitution rules (49)–(51) resembling those of quantum mechanics, but taking into account the fact that space is discretized.

Since the phenomena which hold a central place in this paper are due to the discrete-space nature of numerical wave propagation, they must also be present in many of the other (physical) periodic structures in which wave propagation has been analysed in great detail, and similar theoretical properties must apply. That no such results have been reported in the relevant literature may be attributed in part to the fact that some of the most vivid evidence of quantum-like phenomena in numerical computing manifests itself in experiments with non-uniform grids (as illustrated by the results of Section 8 and by the references in Sections 5 and 10 to wave trapping' in large aerodynamics numerical codes): while non-uniform periodic structures are very common in numerical computing, their occurrence in physical systems is quite rare, and the analysis of wave propagation in classical periodic structures has been devoted almost exclusively to piecewise uniform systems. It is also the case that physical systems do not allow for

experiments to be created and for the corresponding data to be measured with the same ease and accuracy as in numerical computing. Nevertheless, nothing in the new theory prohibits its applicability to equivalent physical structures (that this is indeed the case has been verified, albeit by numerical simulation to support the theory, and will be reported separately). There are of course many precedents for this role of computing in the discovery and investigation of new mathematical concepts and physical phenomena: see for instance Zabusky[24] for an interesting account of the discovery of solitons, which followed the now famous Fermi–Pasta–Ulam computer experiments with the discrete-space analogue of a non-linear vibrating string.

Our analysis has been carried out with (1) as a model of a discrete propagating medium, about the simplest one may find. The results may, with little modification, be made to describe solutions of discrete analogues of the second-order wave equation (5). Strings of lumped masses, which are governed by such discretized equations, have often been described in the literature, in fact as far back as in papers by Johann Bernoulli dating from the first half of the eighteenth century. But one must note, in that respect, that the quantities which are found to play the role of the wave kinetic and potential energies in the new theory are not the analogues of the classical Lagrangian kinetic and potential energies of the corresponding strings of lumped masses. We also note that other discretizations of hyperbolic equations may create periodic structures with interesting new properties. For instance, a finite element–Galerkin discretization of either (3) or (5) generates structures in which left-going and right-going 'particles' with the same energy have different speeds.

REFERENCES

1. G. Browning, H. O. Kreiss and J. Oliger, 'Mesh refinement', *Math. Comput.*, **27**, 29–39 (1973).
2. G. W. Hedstrom, 'Models of difference schemes for $Ut + Ux = 0$ by partial differential equations', *Math Comput.*, **29**, 969–977 (1975).
3. H. Kreiss and J. Oliger, 'Methods for the approximate solution of time dependent problems', *GARP Publication Series No. 10*, World Meteorological Organization, Geneva, 1973.
4. L. N. Trefethen, 'Group velocity of finite difference schemes', *SIAM Rev.*, **23**, 113–136 (1982).
5. R. Vichnevetsky, 'Energy and group velocity in semi-discretizations of hyperbolic equations', *Math. Comput. Simul.*, **23**, 333–343 (1981).
6. R. Vichnevetsky, 'Propagation through numerical mesh refinement for hyperbolic equations', *Math. Comput. Simul.*, **23**, 344–353 (1981).
7. R. Vichnevetsky, 'Group velocity and reflection phenomena in numerical approximations of hyperbolic equations', *J. Franklin Inst.*, 307–330 (1983).
8. R. Vichnevetsky, 'Propagation and spurious reflection in finite element approximations of hyperbolic equations', *Comput. Math. Appl.*, **11**, 733–746 (1985).
9. R. Vichnevetsky, 'Wave propagation analysis of difference schemes for hyperbolic equations: a review', *Int. j. comput. methods fluids*, 409–452 (1987).
10. R. Vichnevetsky and J. B. Bowles, *Fourier Analysis of Numerical Approximations of Hyperbolic Equations*, SIAM (Studies in Applied Mathematics Series), Philadelphia, PA, 1982.
11. M. B. Giles and W. T. Thompkins, Jr., 'Propagation and stability of wavelike solutions of finite difference equations with variable coefficients', *J. Comput. Phys.*, **58**, 349–360 (1985).
12. R. C. Y. Chin and G. W. Hedstrom, 'Scattering of waves from a staggered difference scheme on a variable grid', *Proc. 10th IMACS World Congress*, Montreal, 1982.
13. R. Vichnevetsky, 'Wave propagation and reflection in irregular grids for hyperbolic equations', *Appl. Numer. Math.*, **2**, 133–166 (1987).
14. R. Vichnevetsky, 'Invariance theorems concerning reflection at numerical boundaries', *J. Comput. Phys.*, **63**, 268–282 (1986).
15. R. Vichnevetsky, 'The analogy between numerical wave propagation and quantum mechanics', in D. Lee *et al.* (eds), *Computational acoustics, Vol. 1*, North-Holland, 1988.
16. G. B. Whitham, *Linear and Nonlinear Waves*, Wiley, 1974.
17. H. Goldstein, *Classical Mechanics*, Addison Wesley, 1950.
18. A. d'Abro, *The Rise of the New Physics*, Dover Publications, 1952.
19. A. Messiah, *Quantum Mechanics*, Wiley, 1959.
20. H. J. Pain, *The Physics of Vibrations and Waves*, 3rd Edn, Wiley, 1983.

21. R. Vichnevetsky and E. C. Pariser, 'Non reflecting upwind boundaries for hyperbolic equations', *Numer. methods partial differential equations*, **2**, (1986).
22. C. Cohen-Tadoudji, B. Diu and F. Laloe, *Quantum Mechanics*, Wiley, 1977.
23. P. M. Morse and H. Feshback, *Methods of Theoretical Physics, Vol. II*, McGraw–Hill, 1953.
24. N. J. Zabusky, 'Computational synergetics and mathematical innovation', *J. Comput. Phys.*, **41**, 195–249 (1981).